Chloride Ion Penetration into Cracked UHPFRC During Wetting-drying Cycles

Ana Mafalda Matos, Sandra Nunes, Stefan Chaves Figueiredo, Erik Schlangen, and José L. Barroso Aguiar

Abstract The subject of this paper is the extent to which, during wetting–drying cycles, chloride ions can penetrate Ultra-high-Performance Fibre Reinforced Cementitious Composites (UHPFRC) specimens subjected to combined mechanical and environmental load. Pre-cracking was obtained by subjecting prismatic specimens ($40 \times 40 \times 60 mm^3$) to four-point bending until a predefined crack opening displacement (COD) is reached, using a dedicated test setup. Three target CODs were studied: 300, 350 and 400 µm. Exposure to a concentrated chloride solution (3.5% NaCl) was used as an environmental load. Specimens we subjected to wetting–drying cycles for one year. After this exposure period, the chloride penetration was characterised both qualitatively (by colourimetric analysis with silver nitrate) and quantitatively (by determining the chloride profile). The effect of damage level on chloride penetration and its impact on structures durability is discussed in the current paper.

Keywords Ultra-high-performance fibre reinforced cementitious composites (UHPFRC) · Cracking · Chloride exposure · Durability

A. M. Matos · S. Nunes (✉)
CONSTRUCT-LABEST, Faculty of Engineering (FEUP), University of Porto, Porto, Portugal
e-mail: snunes@fe.up.pt

S. C. Figueiredo · E. Schlangen
MICROLAB, Faculty of Civil Engineering and Geosciences, Delft University of Technology, Delft, The Netherlands

J. L. B. Aguiar
School of Engineering, University of Minho, Guimarães, Portugal

I. B. Valente et al. (eds.), *Proceedings of the 3rd RILEM Spring Convention and Conference (RSCC 2020)*, RILEM Bookseries 33,
https://doi.org/10.1007/978-3-030-76551-4_21

1 Research Scope

The design of UHPFRC aims at a densely compacted cementitious matrix (herein referred as UHPC) using a high content of reactive powders, a minimal amount of water, a high-range water reducer and an adequate fine aggregate gradation, in order to produce high flowability and improved mechanical and durability properties [1]. This superior mechanical and durability performance of UHPFRC makes it particularly suitable for use in rehabilitation and strengthening of reinforced concrete structures. This concept relies on the casting of thin layers/jackets of UHPFRC to strengthening and waterproofing a specific structural concrete element [2].

UHPFRC is being utilized in several applications around the world [3, 4], but it still faces some challenges for broader implementation. In this context, a PhD research programme was developed at the Faculty of Engineering, Porto University, Portugal (FEUP), addressing some of those issues, namely:

- Developing a new UHPC mixture for rehabilitation/strengthening applications employing local available raw materials (including waste materials) and on-site fabrication under regular casting and curing conditions [5]
- To mitigate autogenous shrinkage of UHPC employing internal curing, in order to minimise the early ages cracking risk [5]
- To investigate several critical durability aspects of the new UHPC mixture and compare its performance to other UHPCs reported in the literature
- Studying the influence of cracking on key durability parameters, such as water transport by capillary suction [6] and chloride ion penetration.

Whereas most common commercially-available UHPCs involve high contents of silica fume and thermal curing, the UHPC under study does not. Another distinctive characteristic is that it incorporates a waste generated from oil refinery industry (ECat), acting as an internal curing agent [5].

The current paper focuses on the influence of cracking on chloride ion penetration, in view of the rehabilitation/strengthening applications. UHPFRC small beams, with a typical fibre content of 3.0%, were pre-cracked using a four-point bending test. Different crack patterns were obtained on the specimen's tensile face. Then specimens were subjected to wetting–drying cycles, using a concentrated chloride solution (3.5% NaCl), during one year. After this exposure period, the chloride penetration was characterised both qualitatively (by colourimetric analysis with silver nitrate) and quantitatively (by determining the chloride profile).

2 Experimental Programme

2.1 UHPFRC Mix Proportions, Specimens Manufacturing and Curing

The new UHPFRC recently developed [5] is constituted by CEM I 42.5R Portland cement complying with EN 197-1; silica fume (specific surface area of 19632 m^2/kg; SiO_2 content >90%) fulfilling the requirements of EN 13263-1; limestone filler (specific surface of 550 m^2/kg; $CaCO_3$ > 98%), complying with the requirements of EN 12620; siliceous natural sand (0–1 mm) and ECat (a spent equilibrium catalyst, generated by Sines Refinery, Portugal). A polycarboxylate type superplasticiser with a specific gravity of 1080 kg/m^3 and 40% solid content and potable water were included. As reinforcement, 3.0% by volume of smooth short steel fibres (13 mm length and 0.21 mm diameter) and 2750 MPa of tensile strength were used. Table 1 presents the mixture proportions of the new UHPFRC. More details concerning the origin and properties of raw materials can be found elsewhere [5].

UHPFRC mixtures were produced using a mixer as specified in with NP EN 196-1 following the mixing procedure described in [5]. Several prismatic specimens ($40 \times 40 \times 160$ mm^3) were moulded in one lift without any mechanical vibration due to the self-compacting ability of the mixtures. The number of specimens produced for each condition is detailed in Table 2. The specimens were then covered with a plastic sheet and demoulded after one day, and then kept underwater in a chamber at 20 ± 2 ºC until the testing age.

The referencing of specimens considered the fibre content, the target COD and the specimen replicate number. For example, "3.0%-350-1", corresponds to a specimen number one, incorporating 3.0% steel fibres and a target COD_{load} of 350 µm. Specimens used for assessment of flexural strength at 28 days are referenced as "3.0%-W28-i".

Table 1 Mixture proportions of the new UHPFRC [5]

Material	(kg/m^3)
Cement	690.2
Silica fume	33.6
Limestone filler	250.6
ECat	155.5
Siliceous sand	775.0
Superplasticizer	19.5
Steel fibres	235.0
Mixing water	160.9
ECat's absorption water	46.6

Table 2 Testing plan

References	Conditioning before cracking	Target COD_{load}	Chloride exposure condition	Testing age	Outcomes
3.0%-W28-i	Immersion in water at 20ºC up to 28 days	Test conducted up to failure	none	28 days	Load-displacement curves
3.0%-0-i		0 µm	Unloaded	379 days	Chlorides content profile and penetration depth
3.0%-300-i		300 µm	Loaded	379 days	
3.0%-350-i		350 µm	Unloaded	379 days	
3.0%-400-i		400 µm	Unloaded		

2.2 Cracking Method and Loading Strategy

After 28 days of water curing, prismatic specimens were cracked by imposing different crack open displacements (COD), namely, 300, 350 and 400 µm, through four-point bending loading, according to the procedure described in EN 12390-5 (Fig. 1). The test was carried out employing an Instron 300 kN Instron testing machine, under displacement control with a displacement rate of 0.003 mm/s. Two linear variable differential transducers (LVDT) were fixed on each side of the specimen, perpendicular to the loading direction, to monitor the COD (Fig. 1). When the target COD was achieved (COD_{load}), the specimens "3.0%-350-i" and "3.0%-400-i" were unloaded, and the residual COD was recorded (COD_{res}).

In the specific case of "3.0%-300-i" specimens, when the predefined COD_{load} = 300 µm was achieved, the specimens were unloaded and taken out from

Fig. 1 Four-point bending test cracking method

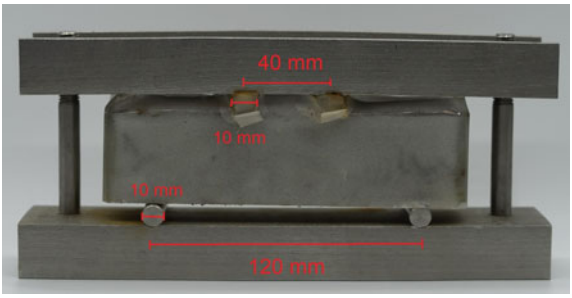

Fig. 2 Illustration of the loading device

the testing machine. Then, these were immediately allocated on a stainless-steel frame, as shown in Fig. 2, while keeping the LVDTs on the specimens. Subsequently, the specimens were re-loaded up to the predefined COD_{load} of 300 µm using threaded rods tightened by a torque wrench. Afterwards, LVDTs were removed carefully, and the wetting–drying chlorides cycles were carried out for these specimens in a loaded state.

Before initiating the wetting–drying cycles, the side and compression surfaces of all prisms were sealed using waterproof tape to ensure the chloride penetration only through the cracked surface. Is must be noted that it was not possible to protect the loaded surfaces of specimens kept in the stainless-steel frame (3.0%-300-i).

2.3 *Characterisation of the Crack Pattern Produced by Bending*

After cracking, a mesh was drawn in the zone of maximum tension strain (in between the two applied forces) (Fig. 3a) in all specimens except those from 3.0%-300-i series. The widths of cracks observed in the tension face of each specimen were measured using a Microscope Multizoom Nikon AZ100 in the unloaded state. Measurements were taken from cracks crossing the three lines A, B and C, as shown in Fig. 3a. A typical photo of a crack with measurements is shown in Fig. 3b.

2.4 *Wetting–Drying Chloride Cycles*

For the long term chloride experiment the "3.0%-0-i" (non-cracked), "3.0%-300-i" (loaded, kept inside the stainless steel frame), "3.0%-350-i" and "3.0%-400-i" (unloaded, with residual COD) specimens were tested, as described in Table 2. Specimens were subjected to weekly wetting–drying cycles consisting of 48 h

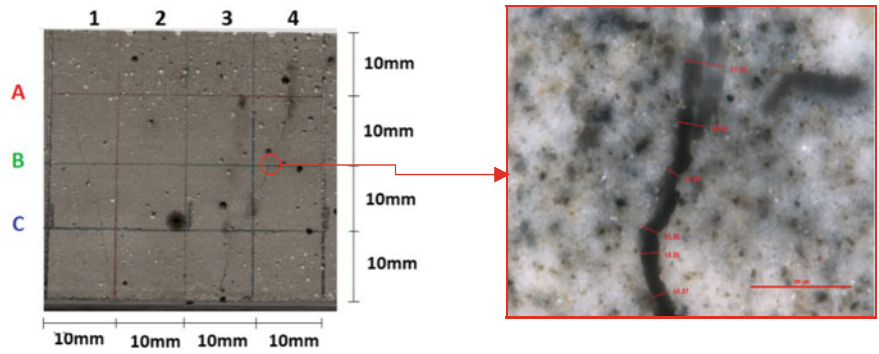

Fig. 3 **a** Scheme for measuring of the crack number and widths; **b** Typical photo with measurements of crack width

partial immersion in a 3.5% NaCl water solution, followed by five days of drying at 20ºC and 50%RH, for 1 year.

2.5 Chloride Penetration Analysis

After the exposure to chlorides, the chloride penetration depth was measured on dry cut specimens surface, using the colourimetric method. A silver nitrate solution was sprayed on the specimen's surface, the chloride depth was measured from the visible white silver chloride precipitation. The other half of the specimen was used for chemical analysis to determine the chloride content following the procedure described in EN 196-2. The samples were taken from the central part of the specimen (in between the two load points) in the direction of chloride penetration close to a macro-crack (when visible), and following the "dry drilling method" procedure according to RILEM Recommendation TC 178-TMC [7], in steps of approximately 5 mm. The steel fibres were removed from the powder sample using a magnet. The chloride content profile was also determined on a water-cured specimen not exposed to external chlorides (C_0).

3 Results and Discussion

3.1 COD Recovery After Unloading (COD_{load} and COD_{res})

Figure 4a shows the load–displacement curves obtained while establishing target COD_{load}, as well as, the curves of specimens tested under four-point bending up to

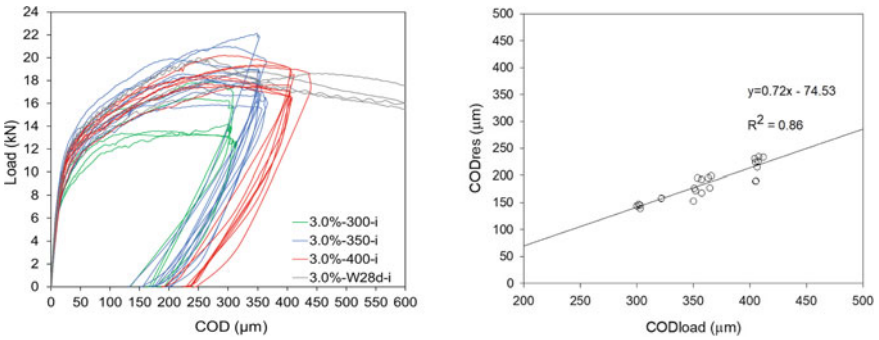

a) b)

Fig. 4 **a** Load-displacement curves obtained at 28 days while establishing target COD_{load} of 300, 350 and 400 µm; and **b** relation between COD_{load} and COD_{resn}

the beginning of softening region, at 28 days (grey lines in Fig. 4a). Results of COD_{res} obtained after unloading as a function of COD_{load} are represented in Fig. 4b, displaying a good linear relation between COD_{res} and COD_{load}. This trend is in agreement with studies of Ma et al. [8] and also with previous studies carried out by the authors [6].

3.2 Crack Pattern Produced by Bending

The average number of cracks observed over a length of 40 mm remained below 9 (see Fig. 5a) while the median of crack width results is under 32 µm (see Fig. 5b, black marks). These results agree with previous findings of the authors [6]. The maximum crack width (see Fig. 5b, red marks) results seem to increase with the increase of COD_{res}.

3.3 Chloride Penetration

After one year of wetting–drying chlorides cycles, all specimens were in excellent condition with no evidence of surface scaling or additional cracking. Nevertheless, as expected, the corrosion of fibres closer to the surface was observed.

For cracked specimens, 3.0%-350-i and 3.0%-400-i, two zones can be distinguished: the zone close to the macro-crack (D_{crack}) and the remaining zones in between the loading points (D_m) with only fine micro-cracks as depicted in Fig. 6. The powder sample for chloride content determination was always extracted near the macro-crack zone. In the cracked specimens (3.0%-350-i and 3.0%-400-i), a localised and significant chloride penetration (between 10 and 17 mm) was

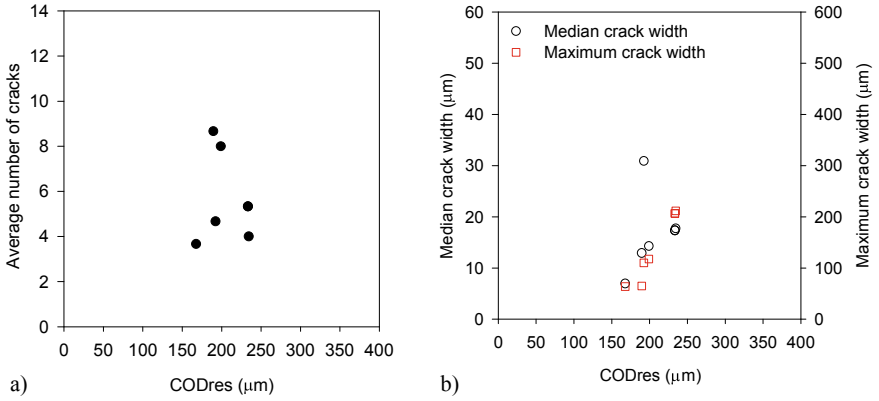

Fig. 5 **a** Average number of cracks and **b** relationship between COD_{res} and median/maximum crack width

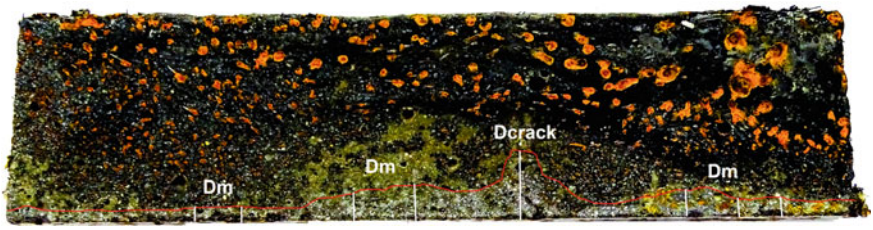

Fig. 6 Chloride penetration on a specimen with a macro-crack formation (3.0%-350-i)

observed close to the macro-crack. On the other hand, in reference specimens or uncracked areas of specimens (similar to D_m), more uniform penetration occurred (roughly 2–3 mm).

Concerning loaded-cracked specimens, 3.0%-300-i, a different chloride penetration pattern was observed, since these specimens present only micro-cracks. These micro-cracks promoted suction of aqueous chloride solution, giving rise to a maximum chloride penetration depth of 18–19 mm.

The average chloride content profiles are presented in Fig. 7. The chloride content is expressed as the percentage of chloride ions by the mass of the sample (UHPFRC without steel fibres). The non-cracked specimens (3.0%-0-i, Fig. 7) showed a high chloride concentration close to the specimen's surface with a decreasing tendency towards the inner part of the specimen. These results are in agreement with the colourimetric analysis with silver nitrate. The maximum chloride content varied between 0.47 and 0.79% at a depth ranging from 0 to 5 mm, then, between 5 and 10 mm depth, the chloride content drastically decreased (around 50%) for values between 0.26 and 0.41%. Afterwards, chloride content kept decreasing with an asymptotic shape converging to 0.20%.

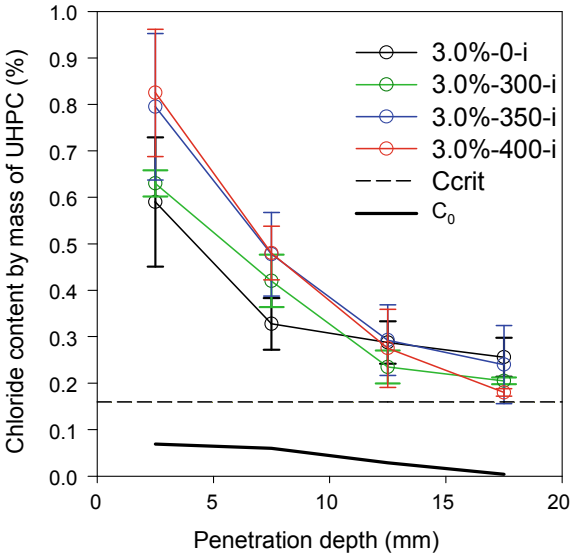

Fig. 7 Chloride profiles

On cracked-unloaded specimens, 3.0%-350-i and 3.0%-400-i, samples were taken near a macro-crack, and it seems that the chloride profiles are similar despite the different COD_{load} applied. Maximum chloride content takes place close to the surface and then decreases as the penetration depth increases. The maximum chloride content, near the surface, varied between 0.61–0.98% and 0.62–0.90% for 3.0%-350-i and 3.0%-400-i specimens, respectively. It is common practice to discard the first mm of a chloride profile and take the next increment, around the 10 mm depth, as a constant initial, pseudo surface concentration [9]. Thus, Fig. 8 illustrates the results of chloride content at 5–10 mm depth as a function of maximum crack width. The chloride content seems not to change significantly with the maximum crack width. However, more data would be necessary to find a clear tendency.

On cracked-loaded specimens, 3.0%-300-i, the maximum chloride content in the cracked area was 0.61–0.65%. The 3.0%-300-i specimens presented also improved behaviour in terms of resistance to ingress of chlorides, compared to the remaining cracked specimens, which might be explained by the occurrence of self-healing. After the first wetting–drying cycles the fine micro-cracks sealed, which slowed the chlorides ingress.

European standard EN 206-1 restricts the chloride content to 0.40% by mass of binder for reinforced concrete structures. The critical chloride content (Ccrit) suggested in EN 206-1 is depicted in Fig. 8 (black dash line), which corresponds to a Ccrit = 0.16% by mass of UHPC. Non-cracked specimens (Fig. 7, black line) presented significant content of chlorides, higher than Ccrit = 0.16% up to 20 mm depth. Besides, the chloride content assessed on the main (and visible) crack of specimens 3.0%-300-i, 3.0%-350-i and 3.0%-400-i revealed that up to a depth of

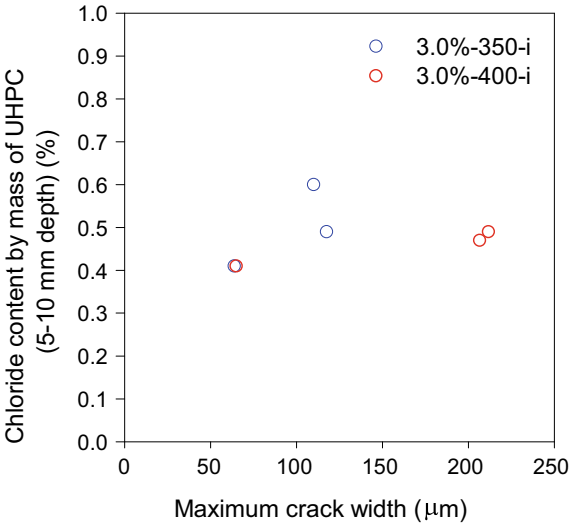

Fig. 8 Relationship between chloride content (5–10 mm depth) with maximum crack width

20 mm, the chloride content was above 0.16%. Though, it shows a decreasing tendency for higher depths.

Based on the results from this experimental campaign only, one can conclude that a minimum of 20 mm cover to reinforcement might be necessary to avoid rebar corrosion. This would be feasible considering the typical thickness of new UHPFRC reinforcement layers, of 40–80 mm [10].

Nevertheless, it should be pointed that: (i) this Ccrit value suggested in EN 206-1 is not a proper chloride threshold value, but rather a practical limit value for the production of fresh concrete [11]; (ii) wetting–drying cycles in laboratory environment can be more severe than "in-situ" exposure to normal ambient conditions (temperature, humidity, carbonation, seawater composition) and the influence scale factors must also be considered. Field experiments are crucial for calibration purposes of laboratory tests or modelling, but very time-consuming and not compatible with the typical duration of a PhD project.

4 Conclusions

After 1-year chlorides exposure, UHPFRC specimens were in excellent condition. However, through the colourimetric test, a penetration depth of approximately 10–19 mm was found on the main crack surrounding area. On the other hand, in non-cracked regions, the penetration depth was of about 2–3 mm, which was similar to the penetration over non-cracked specimens (3.0%-0-i).

EN 206-1 standard suggests a Ccrit equal to 0.40% by mass of binder (cement plus type II additions), which is equivalent to 0.16% by mass of UHPC under study.

Chloride contents observed in this experimental campaign were superior to Ccrit = 0.16% by mass of UHPC up to 20 mm, particularly, near a macro-crack of specimens 3.0%-350-i" and "3.0%-400-i".

Based on this campaign results only, a UHPFRC cover of at least 20 mm would be recommended. However, it should be considered that accelerated testing in the laboratory can be more severe than the exposure of real structures to natural ambient conditions. Thus, real field tests would be necessary to calibrate laboratory results.

Acknowledgements This work was financially supported by: Base Funding—UIDB/04708/2020 and Programmatic Funding—UIDP/04708/2020 of the CONSTRUCT—Instituto de I&D em Estruturas e Construções—funded by national funds through the FCT/MCTES (PIDDAC); by the project POCI-01-0145-FEDER-031777—"UHPGRADE—Next generation of ultra-high performance fibre-reinforced cement-based composites for rehabilitation and strengthening of the existing infrastructure" funded by FEDER funds through COMPETE2020—Programa Operacional Competitividade e Internacionalização (POCI) and by national funds (PIDDAC) through FCT/MCTES; and by FCT—Fundação para a Ciência e a Tecnologia through the PhD scholarship PD/BD/113636/2015, attributed within the Doctoral Program in Eco-Efficient Construction and Rehabilitation (EcoCoRe). Stefan Chaves Figueiredo would like to acknowledge the funding from Science without Borders from the National Council for Scientific and Technological Development of Brazil (201620/2014-6). Collaboration and materials supply by Sines Refinery/Galp Energia, Secil, Omya Comital, Sika, Bekaert and EUROMODAL is gratefully acknowledged.

References

1. Wang, D., Shi, C., Wu, Z., Xiao, J., Huang, Z., Fang, Z.: A review on ultra high performance concrete: Part II. hydration, microstructure and properties. Constr. Build. Mater. **96**, 368–377, Oct (2015)
2. Azmee, N.M., Shafiq, N.: Ultra-high performance concrete: from fundamental to applications. Case Stud. Constr. Mater. **9**, e00197, Dec (2018)
3. Bruhwiler, E., Denarie, E.: Rehabilitation and strengthening of concrete structures using ultra-high performance fibre reinforced concrete. Struct. Eng. Int. **23**(4), 450–457, Nov (2013)
4. Fehling, E., Schmidt, M., Walraven, J., Leutbecher, T., Frohlich, S.: Ultra-high performance concrete UHPC: fundamentals, design, examples. Ernst & Sohn, Wiley, Berlin, Germany (2014)
5. Matos, A.M., Nunes, S., Costa, C., Barroso-Aguiar, J.L.: Spent equilibrium catalyst as internal curing agent in UHPFRC. Cem. Concr. Compos. **104**, 103362, Nov (2019)
6. Matos, A.M., Nunes, S., Aguiar, J.L.B.: Capillary transport of water in cracked and non-cracked UHPFRC specimens. J. Adv. Concr. Technol. **17**(5), 244–259, May (2019)
7. Vennesland, Ø., Climent, M.A., Andrade, C.: Recommendation of RILEM TC 178-TM. Testing and modelling chloride penetration in concrete. Methods for obtaining dust samples by means of grinding concrete in order to determine the chloride concentration profile. Mater. Struct. Constr. **46**(3), 337–344 (2013)
8. Ma, Z., Zhao, T., Yao, X.: Influence of applied loads on the permeability behavior of ultra high-performance concrete with steel fibers. J. Adv. Concr. Technol. **14**(12), 770–781 (2016)
9. Broomfield, J.P.: Corrosion of steel in concrete. Understanding, investigation and repair, 2nd ed. Taylor & Francis (1997)

10. Wassmann, K., Brühwiler, E., Lunk, P.: Strengthening of RC slabs using UHPFRC—concepts and applications. In: 4th International Symposium on Ultra-High Performance Concrete and High-Performance Materials (2016)
11. Angst, U., Elsener, B., Larsen, C.K., Vennesland, Ø.: Critical chloride content in reinforced concrete—a review. Cem. Concr. Res. **39**(12), 1122–1138, Dec (2009)